Astron. Astrophys. 333, L9–L12 (1998)

ASTRONOMY AND ASTROPHYSICS

LETTER

Letter to the Editor

ISOCAM images of the 'elephant trunks' in M 16⋆

Göran L. Pilbratt[1], Bruno Altieri[2], Joris A.D.L. Blommaert[2], C.V. Malcolm Fridlund[1], Jan A. Tauber[1], and Martin F. Kessler[2]

[1] ESA Astrophysics Division, Space Science Department, ESTEC, P.O. Box 299, 2200 AG Noordwijk, The Netherlands
[2] ISO Science Operations Centre, ESA Astrophysics Division, VILSPA, P.O. Box 50727, E-28080 Madrid, Spain

Received 13 November 1997 / Accepted 24 February 1998

Abstract. We have used ISOCAM to obtain images of the 'elephant trunks' in the M 16 'Eagle nebula' in the two broadband filters LW2 (5−8.5 μm) and LW3 (12−18 μm). These pillars are clearly seen in both our filters, their emission has a colour temperature in the range 250−320 K.

We have also detected bright extended emission in the LW3 filter, in an area outside the 'elephant trunks', and with no LW2 counterpart.

We report the detection of a deeply embedded source, presumably connected with M16-E31, which we identify as a YSO. However, to our levels of angular resolution and sensitivity we cannot, in general, correlate discrete sources with the EGGs discovered by the HST. Our observations are consistent with a relatively low level of ongoing low-mass star formation, a fact which may be related to disk disruption taking place at early times in M 16.

Key words: Stars: formation – ISM: clouds – ISM: individual objects: M 16 – Infrared: ISM: continuum

1. Introduction

The H II region M 16 (NGC 6611), the 'Eagle nebula', is an area of active star formation; it contains young massive stars and many intermediate mass (and thus presumably even more low mass) pre-main sequence (PMS) stars (e.g. Hillenbrand et al. 1993 − hereafter Hi93). Striking cloud protrusions − 'elephant trunks' − illuminated by nearby young stars are the result of the interaction between young massive stars with the environment responsible for their formation. These pillars are also, in turn, believed to be regions of star formation themselves.

The interface between the pillars and the H II region has been studied in detail by Hester et al. (1996 − hereafter He96) using the Hubble Space Telescope (HST). A population of small cometary globules, labelled 'evaporating gaseous globules' (EGGs), were discovered to be emerging through the photo-evaporative interface; 73 such EGGs were identified. They are interpreted as density enhancements that have survived against photo-evaporation longer than their less dense surroundings; some are still connected to the parental cloud by material presumably still 'shielded' by them. From a comparison with K-band data (of Hi93) He96 concluded that in some cases EGGs appear to be associated with young stellar objects (YSOs) and, thus, that these EGGs indeed literally are 'hatching' sites of stars. He96 stressed that the fraction of EGGs containing YSOs is unknown.

From adaptive optics K-band observations covering only a fraction of the HST field Currie et al. (1996), with one exception, fail to associate density enhancements identified in the HST images with K-band protostar signatures. Recently McCaughrean (1997 − hereafter McC97) obtained near-IR (NIR) JHK′ imaging of the HST field in M 16. McC97 concluded that only some 20 % of the EGGs might contain young stars, and noted that the proplyds in Orion, which He96 suggest may be objects similar to the EGGs but viewed at a different angle, almost always do have associated NIR stars.

The present Infrared Space Observatory (ISO, e.g. Kessler et al. 1996) observations were obtained in an attempt to assess whether the EGGs discovered by He96 do contain forming stars (as proplyds appear to), and to search for the signatures of YSOs inside the elephant trunks and in the 'base' of these structures.

2. Observations and data reduction

The present ISO observations took place on 19 April 1997, using the long wavelength (LW) array of the ISO camera (ISOCAM, Cesarsky et al. 1996). Raster images were obtained of a field completely covering the HST M 16 field in the two broadband filters LW2 (5−8.5 μm) and LW3 (12−18 μm). With our choice of observing parameters (cf. Table 1) we obtained a raster overlap of half the array FOV in both directions for LW3, and in one direction for LW2. The rastering was performed along the satellite axes.

Send offprint requests to: gpilbratt@astro.estec.esa.nl

⋆ Based on observations with ISO, an ESA project with instruments funded by ESA Member States (especially the PI countries: France, Germany, the Netherlands and the United Kingdom) with the participation of ISAS and NASA.

Table 1. Observing parameters; PFOV is pixel field of view, the ISOCAM LW detector array has 32×32 pixels. N_{exp} is the number of images obtained in each raster position, T_{int} is the integration time for each of these images.

Filter	'Effective' λ	PFOV	Step size
LW2	$6.7\,\mu$m	$1\farcs5$	$24'' \times 48''$
LW3	$14.3\,\mu$m	$3''$	$48'' \times 48''$
Filter	Raster steps	T_{int}	N_{exp}
LW2	9×5	2.1 s	16
LW3	5×5	2.1 s	20

The CAM Interactive Analysis (CIA) software package was used for data reduction (Ott et al. 1997). The raw data images were corrected for dark current using the ISOCAM calibration library ('Cal-G') dark image scaled using a relatively dark region of the LW2 image to minimise the residual dark pattern. The dark image obtained was also used for our LW3 image.

Cosmic ray hits were eliminated from the data by means of the so-called 'Multi-resolution Median Transform' method. The 'IAS model' transient correction (cf. Abergel et al. 1996) was used to correct for detector memory effects in the images, eliminating remnants of strong sources from subsequent raster positions.

Flatfielding was performed using a median filtered flatfield derived from our data, offering a smaller spatial noise than the 'Cal-G' library flatfield. The images at each raster pointing were coadded and sky projected, and finally the raster map image was constructed. No detector field distortion correction was applied to the data.

For flux calibration we adopted 2.19 ADU/s per mJy/pixel for LW2, and 1.97 for LW3. Based on the accumulated in-flight experience, with the application of transient corrections included in the data reduction, these values are believed correct to within $\pm$ 10%.

ISOCAM 'raw' astrometry is typically accurate to within $5''$. Identification of two stars in our LW2 image enabled absolute astrometric calibration using the coordinates of these stars (ID 367 and 401 in their Table 1) given by Hi93. The resulting correction applied to the 'raw' astrometry in our LW2 data was $4\farcs7$. The LW3 astrometry was corrected by provisional identification of two discrete sources with the corresponding sources in the LW2 image. This involved a translation of $0\farcs7$ with respect to the 'raw' LW3 astrometry, and was then verified by comparing the global structure in the two images.

3. Images and extended emission

Our LW2 and LW3 images are shown in Figs. 1 and 2, displaying obvious and significant differences in morphology as compared to those of McC97 ($\sim 1-2\,\mu$m) and He96 ($\sim 0.6\,\mu$m). In the optical the pillars are completely opaque, in the NIR portions of them are nearly transparent, whereas in the present data they are seen in emission.

In the LW2 image all three pillars (Π_1, Π_2, and Π_3 from NE towards SW) – so evident in the HST images – are clearly seen. The brightness is strongly enhanced at the head of Π_1 and at the 'ridge' below it. Below the 'ridge' there is a region of very low intensity emission and a bright star (labelled B). There are a number of discrete sources, many but not all outside the extent of the pillars.

The pillar structure is less obvious in the LW3 emission, especially that of Π_3. By comparing with the LW2 image the low emission region with star B can be discerned, but few clear discrete sources. NE of Π_1 there is also an area of extended emission with peak brightness comparable to that of Π_1; it is an unexpected additional LW3 image feature without any LW2 counterpart.

By smoothing the LW2 image to the resolution of the LW3 data, and assuming dust emission with a $\nu^{1.5}$ emissivity law to be dominating in both filters, we compute a colour temperature (T_c) in the range $250-320$ K over the pillars. T_c is high on the heads of Π_1 and Π_2, but it is highest on the 'ridge' connecting these two pillars.

The nature of the unexpected extended bright emission detected NE of Π_1 in the LW3 data is unclear. Using the background brightness in the LW2 image as an upper limit we compute an upper limit $T_c \sim 200$ K. We are currently attempting to obtain spectral information to investigate this feature, and to refine our T_c estimates.

4. Discrete sources

The SADAM software library was used for object extraction and photometry, employing the multi-resolution method developed by Starck et al. (1997). Specifying conservative thresholds, of order 80 discrete sources were listed in the LW2 image and two dozens in the LW3 image. Their flux densities, $S_{6.7}$ and $S_{14.3}$, were computed, and their positions derived. No 'colour correction' was applied to the photometry, i.e. the flux densities were derived assuming source spectra with constant νS_ν across the filter bands. For YSO-like spectra this may cause inaccuracies of 10 % in the derived fluxes, since LW2 and LW3 are broad-band filters. However, for the present observations background subtraction is the dominant factor determining the total number of sources extracted, and the uncertainty in the fluxes derived for each source.

In the areas with the lowest background levels in the LW2 image the weakest detected discrete sources have $S_{6.7} \gtrsim 5-10$ mJy. In areas with brighter extended emission the detection limit is a factor $\gtrsim 2$ higher, depending on the 'compactness' of the source. In the LW3 image the detection limits are higher, since almost the entire image has high background levels.

The LW2 discrete sources appear generally to coincide with relatively bright stars in the NIR, but only rarely are corresponding sources found in our LW3 data. Sources outside the extent of the pillars are expected to have LW3 counterparts only if embedded. Two such objects, labelled I (isolated object N of the

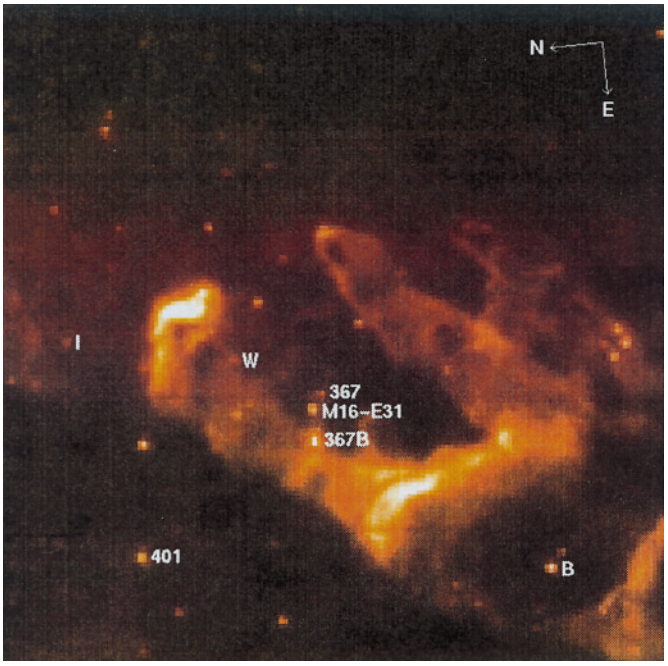

Fig. 1. The LW2 image; the field covered is $4'\times4'$ (160×160 pixels × 1.″5, centered on $\alpha_{\rm J2000} = 18^{\rm h}18^{\rm m}51\overset{\rm s}{.}36$, $\delta_{\rm J2000} = -13^\circ49'48\overset{''}{.}4$. Note pillars (labelled Π_1, Π_2, and Π_3 from NE to SW) and discrete sources.

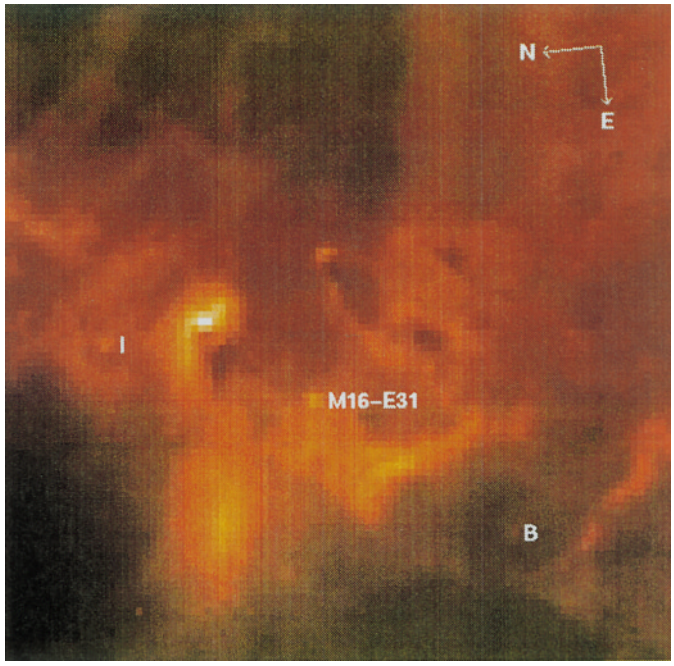

Fig. 2. The LW3 image; the field covered is $4'.8\times4'.8$ (96×96 pixels × 3″), centered on $\alpha_{\rm J2000} = 18^{\rm h}18^{\rm m}51\overset{\rm s}{.}12$, $\delta_{\rm J2000} = -13^\circ49'51''.0$. Note bright emission NE of Π_1.

head of Π_1) and the already mentioned object B, do appear as LW3 sources.

We report the detection of a discrete object close to the tip of a narrow extended protrusion on the SW side of Π_1, this object apparently coincides with M16-E31. Its peak flux is $\sim 50\,\%$ higher than that of the head of Π_2 in both bands, it is unresolved, and in the NIR there is only a faint object visible in this position. Its derived flux densities are $S_{6.7} \sim 50$ mJy and $S_{14.3} \sim 175$ mJy. Forming the colour index $c_i \equiv \log(S_{14.3}/S_{6.7})$ we obtain ~ 0.5; thus it is a very 'red' object indeed. We tentatively identify it (cf. Nordh et al. 1996) as an embedded YSO. Assuming an $\nu^{1.5}$ emissivity law the colour temperature corresponding to the observed $S_{14.3}/S_{6.7}$ ratio is ~ 250 K.

From extensive ISOCAM observations (also using the LW2 and LW3 filters) of the Chamaeleon region (Nordh et al. 1996), and incorporating IRAS data to take colder source components into account, Olofsson et al. (1997) have established an empirical linear relationship between $\log(S_{6.7})$ and $\log(L_{\rm bol})$ for YSOs (defined as having $c_i > -0.3$) valid over 3-4 magnitudes of luminosity. Using their preliminary calibration and assumed distance of 150 pc for Chamaeleon, and adopting a distance to M 16 of 2 kpc (Hi93), it predicts $L_{\rm bol} \sim 2\,L_\odot \times (S_{6.7}/5\,{\rm mJy})$ for M 16. Extrapolating to luminosities just above their highest, we derive a bolometric luminosity of $L_{\rm bol} \sim 20\,L_\odot$ for the YSO connected to M16-E31.

The bright peak 'below' M16-E31 in the LW2 map we identify with source 367B of Currie et al. (1996). It has $S_{6.7} \sim 100$ mJy, however, it is difficult to assign a LW3 flux, thus we cannot positively identify this object as a YSO.

The two other sources detected in both filters mentioned are I and B, both located in areas of low background emission. We derive $S_{6.7} \sim 15$ mJy and $S_{14.3} \sim 40$ mJy giving $c_i \sim 0.4$ and $L_{\rm bol} \sim 6\,L_\odot$ for I, and $S_{6.7} \sim 75$ mJy and $S_{14.3} \sim 45$ mJy giving $c_i \sim -0.2$ and (extrapolated) $L_{\rm bol} \sim 30\,L_\odot$ for B, provided that these objects indeed are embedded YSOs.

We have attempted to correlate discrete sources in our LW2 image with features in the HST image, in particular with the EGGs discussed in He96. To our levels of angular resolution ($1.22\lambda/D = 2\overset{''}{.}8$ and $6\overset{''}{.}0$ corresponding to approximately 6000 AU and 12000 AU) and sensitivity we do not, in general, find such a correlation.

5. Discussion

On morphological grounds the 'elephant trunks' can be thought of as giant versions of the attached EGGs. The opaque patches in the pillar heads in the NIR indicate the density enhancements that are a prerequisite for their formation. The bright 'ridge' and parts of Π_2 are also fairly opaque in the NIR. The head of Π_1 and the bright 'ridge' below it appear much brighter (by a factor $\gtrsim 3$) than e.g. the heads of Π_2 and Π_3 in our images. There are two classes of possible explanations; the difference in brightness could be apparent, due to the geometry, or could be due to intrinsically different emission properties.

The bright observed emission can arise in the interface region between the pillars and the photon field from the nearby early O stars (He96 estimate 2×10^{50} ionizing photons s^{-1} originating at a distance of ~ 2 pc). A small fraction of the intercepted energy already suffices to account for the emission observed in our filter bands. Following He96, Π_1 could be inclined

towards us and Π_2 and Π_3 away from us, with the photon field originating above and in between. In this picture, the illuminated far sides of Π_2 and Π_3 must be attenuated by extinctions in excess of $A_v \sim 100$. However, if Π_2 and Π_3 were $\sim 25\,\%$ more distant from the photon source than Π_1 and the 'ridge', then this requirement could be relaxed to $A_v \sim 50$. This scenario is supported by radio spectral line observations which indicate that the systemic velocities of Π_2 and Π_3 differ from that of Π_1, and that it is unlikely that the extinctions are as high as $A_v \sim 100$ (G. White, private communication).

Alternatively, the bright emission could be due to an unresolved population of warm embedded objects. It is conceivable that a few of the weaker LW2 sources indeed are YSOs but that we are unable to positively identify them as such. An example is object W below the head of Π_1, which also coincides with a faint NIR object. Its flux is $S_{6.7} \sim 25$ mJy, corresponding to $L_{bol} \sim 10\,L_\odot$ using the Olofsson et al. (1997) relation. We conclude that there is no large population of obscured YSOs with $L_{bol} \gtrsim 10\,L_\odot$ outside and over much of the pillars. However, we do make the strong reservation that the limit is (substantially) higher in the bright head and base of Π_1 and in the bright 'ridge' extending towards Π_2, where we would be unable to detect even sources like M16-E31. In the heads of Π_1 and Π_2 there are bright compact objects in the NIR coincident with our positions of peak emission. In the present data, however, the emission is not pointlike, but extended (especially in Π_1), making it difficult to assign fluxes for any potential 'discrete' source components.

The small number of sources found in the observed field is at odds with the usual description of M 16 as a region of active star formation. For comparison, a scan of the Milky Way by Pérault et al. (1996), which avoided very active regions, produced 395 point sources with LW3 in 0.144 deg^2, implying some 65 sources in our 0.004 deg^2 (assuming that the bulk of the emission in the Milky Way scan originates in GMCs at ~ 5 kpc). The total number of sources we find in the M 16 field is low compared to the latter, though still much higher than what would be expected in dark clouds (e.g. the Chamaeleon survey by Nordh et al. (1996) would imply at most one source in our field). This relative paucity of intermediate-temperature sources could be connected to the generally low number of disks found in M 16 (Hi93, He96). Our observations are consistent with the hypothesis put forward by those authors that in this region disk disruption could occur at very early times indeed.

The age inferred for PMS stars in M 16 is 0.25 to 1 million years (Hi93). For an age of 1 million years $10\,L_\odot$ corresponds to stars with $M \sim 2.5\,M_\odot$ (e.g. D'Antona & Mazzitelli 1994), for 0.25 million years the corresponding mass limit is a factor two lower. Assuming a standard Miller & Scalo (1979) initial mass function (IMF), only $\sim 4\,\%$ of all stars forming are more massive than $\sim 2.5\,M_\odot$, and $\sim 10\,\%$ more massive than half this value. Thus, our observations are consistent with ongoing formation of a population of order tens of low-mass stars taking place in this region of M 16, and the conclusions of McC97 about the association between NIR sources and EGGs.

Acknowledgements. We gratefully acknowledge receiving a preprint from Göran Olofsson and a colour image from Mark McCaughrean, and helpful discussions with Laurent Vigroux and Glenn White. The ISOCAM data presented in this paper were analysed using the CIA, a joint development by the ESA Astrophysics Division and the ISOCAM Consortium led by the ISOCAM PI, C. Cesarsky, Direction des Sciences de la Matière, CEA, France.

References

Abergel A. et al. 1996, A&A 315, L329
Cesarsky C.J. et al. 1996, A&A 315, L32
Currie D. et al. 1996, ESO Messenger 86, 31
D'Antona F., Mazzitelli I. 1994, ApJS 90, 467
Hester J. et al. 1996, AJ 111, 2349 (He96)
Hillenbrand L.A., Massey P., Strom S.E., Merrill K.M. 1993, AJ 106, 1906 (Hi93)
Kessler M.F. et al. 1996, A&A 315, L27
McCaughrean M.J. 1997, Orion proplyds and the Eagle's EGGs. In: Reipurth B., Bertout C. (eds) Proc. of IAU Symp. 182, Herbig-Haro Flows and the Birth of Low Mass Stars, p. 551. Kluwer, Dordrecht (McC97)
Miller G.E., Scalo J.M. 1979, ApJS 41, 513
Nordh L. et al. 1996, A&A 315, L185
Olofsson G. et al. 1997, ISOCAM Observations of Young Low-mass Stars. In: Proc. of Brown Dwarfs and Extrasolar Planets Workshop (in press)
Ott S. et al. 1997, Design and Implementation of CIA, the ISOCAM Interactive Analysis System, In: Hunt G., Payne H.E. (eds) ASP Conf. Series Vol. 125, p. 34
Pérault M. et al. 1996, A&A 315, L165
Starck J.-L., Murtagh F., Bijaoui A. 1997, Image Processing and Data Analysis in the Physical Sciences: The Multiscale Approach, Cambridge University Press (in press)